

## THE FIRST *SWIFT* X-RAY FLASH: THE FAINT AFTERGLOW OF XRF 050215B

A.J. LEVAN<sup>1,2</sup>, J. P. OSBORNE<sup>1</sup>, N.R. TANVIR<sup>1,2</sup>, K.L. PAGE<sup>1</sup>, E. ROL<sup>1</sup>, B. ZHANG<sup>3</sup>, M.R. GOAD<sup>1</sup>, P.T. O'BRIEN<sup>1</sup>,  
R.S. PRIDDEY<sup>2</sup>, D. BERSIER<sup>4</sup>, D.N. BURROWS<sup>5</sup>, R. CHAPMAN<sup>2</sup>, A.S. FRUCHTER<sup>6</sup>, P. GIOMMI<sup>7</sup>, N. GEHRELS<sup>8</sup>,  
M.A. HUGHES<sup>2</sup>, S. PAK<sup>2</sup>, C. SIMPSON<sup>9</sup>, G. TAGLIAFERRI<sup>10</sup>, E. VARDOULAKI<sup>11</sup>

*Accepted for publication in ApJ*

### ABSTRACT

We present the discovery of XRF 050215B and its afterglow. The burst was detected by the *Swift* BAT during the check-out phase and observations with the X-ray Telescope began approximately 30 minutes after the burst. These observations found a faint, slowly fading X-ray afterglow near the centre of the error box as reported by the BAT. Infrared data, obtained at UKIRT after 10 hours also revealed a very faint K-band afterglow. The afterglow appears unusual since it is very faint, especially in the infrared, with  $K > 20$  after 9 hours post-burst. The X-ray and infrared lightcurves exhibit a slow, monotonic decay with  $\alpha \sim 0.8$  and no evidence for a steepening associated with the jet break to 10 days post burst. We discuss possible explanations for the faintness and slow decay in the context of present models for the production of X-ray Flashes.

*Subject headings:* gamma-rays: bursts

### 1. INTRODUCTION

X-ray Flashes (XRFs) appear to be a subclass of Gamma-Ray Bursts (GRBs). They have similar durations to the long-soft GRBs, but they have a low gamma-ray flux, a high ratio of X-ray to gamma-ray flux, and a spectral peak at a much lower energy (Kippen *et al.* 2003). First identified by the Wide Field Cameras on BeppoSAX (Heise *et al.* 2001) they have been located with increasing frequency by *HETE-2*. Followup observations have in some cases successfully found afterglow emission, most commonly at X-ray wavelengths, and occasionally in the optical and nIR. Accurate positions have indicated that, like GRBs, XRFs are found in star-forming galaxies at cosmological distances (e.g. Bloom *et al.* 2003), but, based on statistics of a few, at rather lower median redshift than GRBs. Recently the very low-redshift XRF 060218, 145 Mpc distant, was shown to be associated with SN 2006aj (Campana *et al.* 2006; Pian *et al.* 2006; Modjaz *et al.* 2006), clearly demonstrating that some XRFs, as for long duration GRBs originate in

the core collapse of a massive star in a type Ic supernova (Hjorth *et al.* 2003; Stanek *et al.* 2003). Photometric evidence for associated supernovae has also been seen in a number of XRFs previously (e.g. Fynbo *et al.* 2004; Soderberg *et al.* 2004;2005; Bersier *et al.* 2006), however the absence of SN signatures in some cases indicate that the SN emission may be markedly fainter than the prototypical GRB supernova SN 1998bw (Levan *et al.* 2005; Soderberg *et al.* 2005).

The existence of XRFs shows that the range of spectral properties associated with GRBs is very large. The peak of the  $\nu F_\nu$  spectrum ( $E_p$ ) can be seen from  $<5$  keV to  $> 1$  MeV. An important question is, therefore: what physical processes are responsible for this range of energies? Observations of the prompt and afterglow emission of XRFs can be used to probe this question and place constraints on the energy generation and physical structure within these highly energetic explosions.

Various scenarios have been proposed to explain the lower peak energy of XRFs compared to GRBs; these can be split into several subsets of model, of which the most broadly discussed are: (i) GRBs at very high redshifts would have their spectral energy distributions (SEDs) shifted into the X-ray window (Heise *et al.* 2001); (ii) GRBs whose Lorentz factor is modified due to the effects of baryon loading within the jet. In external shock models high baryon loading (the so-called dirty fireball) can create an XRF (Dermer *et al.* 1999; Ramirez-Ruiz & Lloyd-Romero 2002; Huang *et al.* 2002), while in contrast for internal shock models very clean jets produce large X-ray fluxes (Zhang & Meszaros 2002, Barraud *et al.* 2005). (iii) GRBs with either a differing geometry or observer viewing angle can also naturally create XRFs, for example due to broader than normal jets (Huaag *et al.* 2004; Zhang *et al.* 2004); bursts where the line of sight is "off-axis" with respect to the jet orientation or bursts whose jet is structured, either in a simple (two component) manner, or with more complex variations with viewing angle. (iv) Finally it is possible that XRFs represent manifestations of differing physical processes to GRBs themselves, perhaps originating from a hot photo-

<sup>1</sup> Department of Physics and Astronomy, University of Leicester, University Road, Leicester, LE1 7RH, UK

<sup>2</sup> Department of Physics, Astronomy and Mathematics, University of Hertfordshire, College Lane, Hatfield, Herts, AL9 10AB, UK

<sup>3</sup> Department of Physics, University of Nevada Las Vegas, Las Vegas, NV 89154

<sup>4</sup> Astrophysics Research Institute, Liverpool John Moores University, Twelve Quays House, Birkenhead CH41 1LD

<sup>5</sup> Department of Astronomy and Astrophysics, Penn State University, University Park, PA 16802, USA

<sup>6</sup> Space Telescope Science Institute, 3700 San Martin Drive, Baltimore, MD21218, USA

<sup>7</sup> ASI Science Data Center, Via Galileo Galilei, I-00044 Frascati, Italy

<sup>8</sup> NASA/Goddard Space Flight Center, Greenbelt, MD 20771, USA

<sup>9</sup> Astrophysics Research Institute, Liverpool John Moores University, Twelve Quays House, Egerton Wharf, Birkenhead CH41 1LD, UK

<sup>10</sup> INAF-Osservatorio Astronomico de Brera, Via E. Bianchi 46, I-23807, Merate (LC), Italy

<sup>11</sup> Department of Physics, University of Oxford, Denys Wilkinson Building, Keble Road, Oxford OX1 3RH

sphere (Meszaros *et al.* 2002).

The discovery of a correlation between  $E_p$  and the square root of the isotropic energy release ( $E_{iso}$ ) (Amati *et al.* 2002) directly implies that softer bursts have lower energies and can be well explained by models where the XRF is the result of a viewing angle effect. In other words, XRFs are seen when a classical GRB is viewed off the primary collimation so the highest energy emission is not seen (e.g. Yamazaki *et al.* 2002; Rhoads 2003; Dado *et al.* 2004). However, outliers to this relation can be found (e.g. Sazonov *et al.* 2004), and it remains to be confirmed that it is purely the result of a viewing angle effect.

The *Swift* satellite was launched in November 2004 and is now delivering localizations for approximately 2 GRBs per week (see Gehrels *et al.* (2004) for a description of the *Swift* mission). The passband of the GRB detectors on *Swift* is smaller than that on *HETE-2*, with a low energy response down to 15 keV compared with 5 keV for *HETE-2*. XRF 050215B was the first XRF to be detected by *Swift* and to have moderately rapid X-ray followup (previous XRFs have not been observed in X-rays for at least several hours, and more typically days). Here we report the results of optical/IR and X-ray observations of XRF 050215 and the constraints they place on models for the production of XRFs.

## 2. OBSERVATIONS

XRF 050215B was detected by the *Swift* Burst Alert Telescope at 02:33:12 UT on 15th February 2005; the initial location was RA = 11:37:48, Dec = 40:48:18 with a 90% error radius of 4 arcminutes (trigger 106106, Barthelmy *et al.* 2005a). *Swift* slewed to the burst promptly, but was unable to observe until  $\sim 29$  minutes after the trigger because it was in the high radiation environment of the South Atlantic Anomaly. X-ray Telescope observations revealed a faint, slowly fading point source, identified as the X-ray afterglow of XRF 050215B (Goad *et al.* 2005). The UV and Optical Telescope did not yield a detection of any source at the location of this X-ray object (Romig *et al.* 2005a,b).

The burst was also seen by *HETE-2*, and an analysis of this data revealed a best fitting  $E_p = 17.6$  keV, with a 95% upper bound of  $E_p < 30.3$  keV (Nakagawa *et al.* 2005). The ratio of fluxes in the 2-30 and 30-400 keV bands was 1.65, implying significantly more X-ray emission than  $\gamma$ -ray and indicating that 050215B was indeed an XRF.

Initial ground-based observations failed to yield an optical counterpart. The BOOTES-2 wide field camera was observing the field at the time of the burst, limiting the unfiltered magnitude of any flash to  $> 10$  (Jelinek *et al.* 2005). ROTSE-III observations started 100s after the burst, however these images failed to yield an optical counterpart to limiting magnitudes of  $R \sim 17.8 - 18.8$  up to 50 minutes after the burst (Yost *et al.* 2005). Radio upper limits of 93 and 156  $\mu\text{Jy}$  ( $3\sigma$ ) at 2.9 and 12 days after the burst were reported by Soderberg & Frail (2005a,b). A skymap with the location of the burst (and afterglow) is shown in Figure 1.

### 2.1. *Swift* Observations

The *Swift* satellite and its gamma-ray Burst Alert Telescope (BAT), X-ray Telescope (XRT) and UV/Optical

Telescope (UVOT) are described by Gehrels *et al.* (2004), Barthelmy *et al.* (2004, 2005b), Burrows *et al.* (2004, 2005) and Roming *et al.* (2004, 2005c). The *Swift* data described here has been processed with version 2.0 of the *Swift* software<sup>12</sup>, using the standard BAT and XRT pipelines.

The BAT detected XRF 050215B below 150 keV, showing a single peaked lightcurve, (see Figure 2). The rise to peak lasts 2-4 s, while the decline takes 7-10 s. The  $T_{50}$  and  $T_{90}$  and durations are 3.4 and 7.8 seconds, respectively. The BAT trigger time (02:33:43 UT) corresponds to the peak of the light curve. This time was mis-reported initially; all times from the burst stated in this paper use this correct trigger time. A single power-law spectral fit to the entire burst between 15 and 150 keV results in a good fit ( $\chi^2/\text{dof} = 1.0$ ), with a photon power law index of  $2.3 \pm 0.4$ . The total 15-150 keV fluence in the T90 interval is  $2.33 \pm 0.6 \times 10^{-7}$  erg  $\text{cm}^{-2}$  (errors are quoted as 90%). The extrapolated fluence in the 30-400 keV FREGATE region is  $2.0 \times 10^{-7}$  erg  $\text{cm}^{-2}$ , in agreement with the results obtained by Nakagawa *et al.* (2005). While XRF 050215B had a fluence somewhat below the *Swift* average, it is unusual in having a very soft spectrum (corresponding to a 2-30 keV to 30-400 keV extrapolated fluence ratio of  $S_X/S_\gamma = 2.0^{+0.2}_{-0.3}$ ) consistent with the X-ray flash characterisation of Nakagawa *et al.* (2005).

Observations with the XRT began at 03:03:11 UT (approximately 30 minutes after trigger), and continued for 13.3 days; they are detailed in table 1. The first exposure was made in Windowed Timing (WT) mode while all later observations were in Photon Counting (PC) mode; a total of 128 counts were obtained from XRF 050215B. The location of the X-ray afterglow was found to be RA = 11:37:47.66, Dec = 40:47:46.7, with a 90% error radius of 4.4 arcseconds (Moretti *et al.* 2006). The X-ray lightcurve of XRF 050215B is shown in Figure 3 (and is combined with the BAT lightcurve). The WT data were extracted from a box  $94''$  across (40 pixels), with the background measured from the same size region offset from the source. For the PC mode data counts were extracted from a  $47''$  (20 pixel) radius region centred on the source, with the background taken from a source-free region 9 times larger in area. All points in Figure 3 correspond to a better than  $3\sigma$  detection of the source. The X-ray afterglow of XRF 050215B declines as an unbroken power law with a decay index of  $0.82 \pm 0.08$ . With the modest number of XRT counts only limited spectral information can be derived. We fit a power law model to the total PC mode afterglow spectrum (which covers 0.5-2.6 keV), finding a good fit for a photon index of  $1.5 \pm 0.5$  assuming the Galactic absorbing column of  $2 \times 10^{20}$   $\text{cm}^{-2}$ . No excess absorption over that due to our Galaxy is seen; at zero redshift  $\Delta N_H < 3.8 \times 10^{21}$   $\text{cm}^{-2}$  (90%). Examination of the ratio of counts in the 0.3-1.0 keV to 1.0-10 keV bands as a function of time showed no variation. Unabsorbed 0.3-10 keV fluxes at 1 and 11 hours derived from Figure 3 and the spectral parameters above are respectively 28 and  $4.9 \times 10^{-13}$  ergs  $\text{s}^{-1}$   $\text{cm}^{-2}$ .

The *Swift* UVOT also observed the position of XRF 050215B at times coincident with the XRT obser-

<sup>12</sup> <http://heasarc.gsfc.nasa.gov/docs/software/lheasoft/>

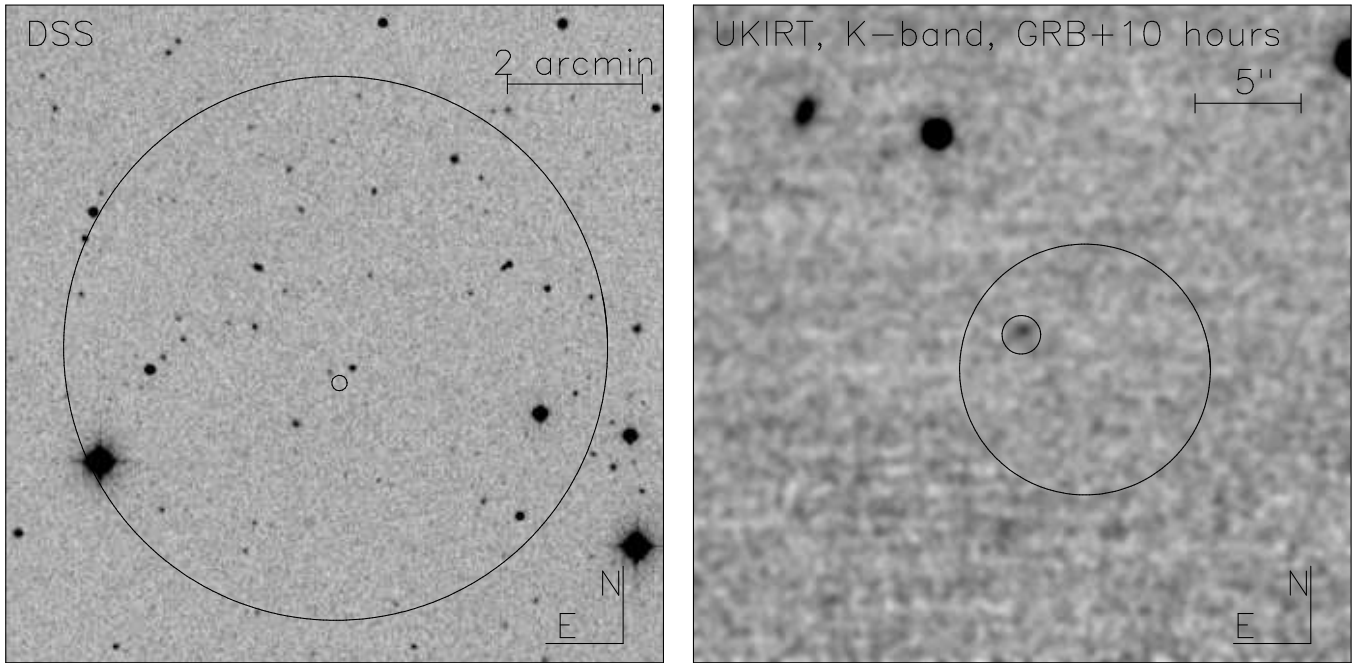


FIG. 1.— The sky position of XRF 050215B. The left hand image shows a region of the Digital Sky Survey (DSSII-red) with the BAT error box marked as the large circle and the XRT position labeled within it. The right hand image shows our first UKIRT observation. The large circle in this image is the XRT location and 90 % confidence region. The location of the IR afterglow is also marked.

observations using its full range of filters. No new source was detected, either initially or later with longer exposures.  $3\sigma$  upper limits include  $U > 20.2$ ,  $B > 20.1$ ,  $V > 19.3$  at 0.57, 0.60, 0.48 hours, and  $V > 21 - 22$  up to 13.3 days after the burst.

## 2.2. Ground based observations

IR images were obtained at UKIRT using the UFTI instrument (Roche *et al.* 2002) in the K98 filter (see Figure 1). Dithered observations were flat-fielded, sky- and dark-subtracted and combined using ORAC-DR (Cavanagh *et al.* 2002). IR and optical images were also taken at Gemini: NIRI data (Hodapp *et al.* 1995) which were also processed with ORAC-DR; GMOS optical data (Hook *et al.* 2004) which were reduced via the specific Gemini/GMOS tasks with IRAF<sup>13</sup>. Additionally a 4 x 30 minutes spectrum of the potential host was taken with GMOS with an R400 grating and the central wavelength varying between 6400 and 6550 Angstrom, from March 11.47 to 11.56 UT. Data reduction was done in a standard fashion using IRAF. Only a very weak continuum was seen, there were no obvious emission lines in the combined spectrum between 6000 and 8500 Angstroms. A complete log of observations is shown in table 2.

Our first image was obtained approximately 10 hours after the burst with a second epoch obtained the following night ( $\sim 33$  hours post-burst). Comparison of these images revealed a fading point source at RA=11:37:47.90, Dec = 40:47:45.6, approximately 33 arcseconds from the centre of the BAT error box and well within the refined XRT position given in section 2.1.

To perform photometry of the afterglow we used an

aperture equal to the FWHM of the images at each epoch. During our UKIRT observations photometric standards were also observed which allowed us to subsequently calibrate the field. The photometric calibration of the R-band images was done using the photometry from the Sloan Digital Sky Survey, which covers the region of the burst in the same filter as used for the GMOS observations.

Photometry of XRF 050215B is shown in table 2 and the K-band light curve is shown in Figure 4. The afterglow was very faint, and therefore the signal to noise was typically low ( $3 - 10\sigma$  in most observations). However the afterglow is clearly fading. A single power-law fit to the K-band data yields a best fit decay slope (fitted as  $F(t) \propto t^{-\alpha}$ ) of  $\alpha = 0.47 \pm 0.08$ , unusually slow for GRB afterglow which fall typically with  $\alpha = 1$  in the first hours to days after the burst, and more rapidly after this. One possibility is that our measured fluxes do not contain pure afterglow but some contribution from an underlying host galaxy. In this case the true decay slope may be faster. We can estimate the maximum possible contribution from an underlying host by making the assumption that the host galaxy contributes a flux equal to the upper limit of the final epoch observation (i.e. lies just below the detection threshold). Given the R magnitude of the host (see below) and the typical R-K colours of GRB host galaxies (in the range 2.5 - 3, Le Floc'h *et al.* 2003) it is unlikely that the host is significantly fainter than this, and therefore this may provide an acceptable estimate of the afterglow decay. The (putative host) subtracted photometry is shown in red in Figure 4. This photometry, while very uncertain, is marginally consistent with a single power-law decay of index  $\alpha = 0.82 \pm 0.08$ ; thus, within the uncertainty (due to the unknown host magnitude), the optical and X-ray slopes are consistent with

<sup>13</sup> For information on ORAC-DR see <http://www.oracdr.org> and for the Gemini IRAF tasks see <http://www.gemini.edu/sciops/data/dataIRAFIndex.html>

TABLE 1  
*Swift* XRT OBSERVATIONS OF XRF 050215B

Start (hours)	End (hours)	Exp. Fraction	Source counts	Background counts	XRT mode
0.498	0.656	1.0	45	16	WT
1.603	1.699	1.0	11	0.22	PC
3.219	3.416	1.0	17	0.56	PC
4.819	5.133	1.0	16	0.67	PC
6.419	6.783	1.0	14	0.89	PC
8.036	8.399	1.0	13	0.56	PC
47.048	66.455	0.081	16	4.6	PC
69.528	93.433	0.14	19	12	PC
95.250	320.572	0.0098	28	16	PC

NOTE. — *Swift* XRT observations of XRF 050215B. A final observation at 13.3 days was too short to be useful, and is not listed here. The start and end times are given in hours since the burst (i.e. hours after 2005-02-15 02:33:12 UT)

being identical.

PSF matched image subtractions of the optical observations taken 11, 21 and 115 days after the burst reveal no evidence for any variation, demonstrating that the optical light from XRF 050215B was dominated by the host galaxy from 11 days onwards, and did not contain a significant contribution from either afterglow or associated supernova (the limit on any transient emission at the location of the afterglow is  $R \sim 25.8$ ). The magnitude of this host galaxy is  $R = 24.7$ , comparable to the median of GRB host galaxies seen to date. Our final K-band point can also be used to place a limit on the host colour. Assuming it has  $K > 22.25$  this implies that  $R - K < 2.5$ . This is again comparable to the  $R - K$  colours of GRB hosts which have a mean  $R - K = 3$  (Chary *et al.* 2002; Le Floc'h *et al.* 2003).

Under the assumption that a supernova was associated with XRF 050215B, we can use the observed limits on the supernova emission to crudely estimate a lower bound to the redshift (also assuming that there is no excess extinction along the line of sight to XRF 050215B). The limiting magnitude of any supernova of  $R = 25.8$  is comparable to the peak magnitude of a supernova such as SN 1998bw at  $z = 1$ . However more typical type Ic supernova such as those putatively associated with XRFs (e.g. Fynbo *et al.* 2004; Bersier *et al.* 2005) span a range of magnitudes from similar to SN 1998bw to a factor of 10 fainter, these fainter supernovae would only be visible to moderate  $\sim 0.5$  redshift.

### 3. DISCUSSION

Figure 5 shows the range of magnitudes seen in the K-band afterglow sample which has been observed to date (Rau *et al.* 2004 and references therein). In addition to the sample determined from GRBs discovered before *Swift* (e.g. *BeppoSAX*, *HETE-2*) which are shown in black, the K-band points from afterglows detected by *Swift* are also shown as dark blue triangles and the highest redshift bursts (GRBs 050814 and 050904) are shown in as green squares. The afterglow of XRF 050215B is shown in red and, as can be seen to be the faintest afterglow observed to date in the K-band (January 2006), and lies toward the faint end of the X-ray afterglow sample (e.g. Nousek *et al.* 2006; O'Brien *et al.* 2006).

It is possible that the faintness of the optical and X-ray afterglow of XRF 050215B could be related to the

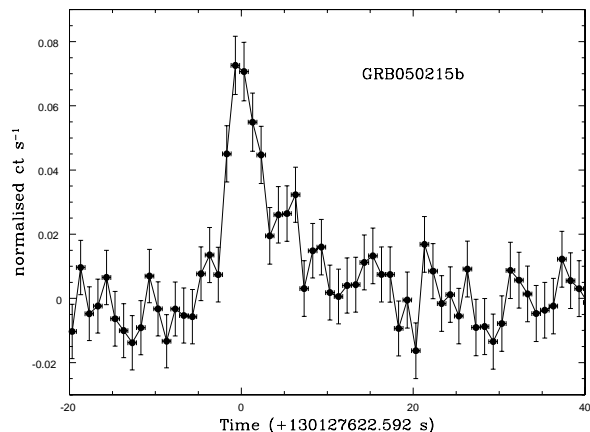


FIG. 2.— The BAT 15-350 keV light curve of the XRF 050215B.

faintness of the prompt emission component. Berger *et al.* (2005) show that typically *Swift* bursts are fainter than those detected by *HETE-2* and *BeppoSAX* at essentially all wavelengths (i.e. both in prompt emission and in X-ray/Optical Afterglows). However XRF 050215B was also detected by *HETE-2* and the fluences observed in the 2-30 and 30-400 keV band were  $2.8 \times 10^{-7}$  ergs and  $1.7 \times 10^{-7}$  ergs, lying between the fluences seen for XRF 020903 and 030723, the XRFs which have the best studied optical afterglows (e.g. Sakamoto *et al.* 2005). The extrapolation of the X-ray afterglow of XRF 050215B out to later times, comparable to those of X-ray observations of previous XRF afterglows, show that it would achieve a 10 day flux of approximately  $1 \times 10^{-14}$  ergs  $s^{-1}$   $cm^{-2}$ , somewhat fainter than the afterglows of XRF 011030 and 020427 at these times (Kouveliotou *et al.* 2004; Levan *et al.* 2005); however it would have been slightly brighter than the afterglow of XRF 030723 (Butler *et al.* 2004). The afterglow decay is, however very shallow - slower than all but four of those studied by O'Brien *et al.* 2006, and, furthermore continues to have a shallow decay for  $\sim 10$  days post burst.

A dusty environment does not seem able to explain the faintness of this burst since it is faint at both X-

TABLE 2  
GROUND BASED OBSERVATIONS OF XRF 050215B

UT	$\Delta t$ (days)	Instrument	Filter/Grating	Seeing (")	Exptime (s)	Magnitude
Feb 15.519	0.413	UKIRT/UFTI	K98	0.42	800	$20.23 \pm 0.11$
Feb 16.497	1.391	UKIRT/UFTI	K98	0.48	1200	$20.75 \pm 0.22$
Feb 17.466	2.360	UKIRT/UFTI	K98	1.05	3000	$21.10 \pm 0.31$
Mar 03.565	16.457	GEMINI/NIRI	K	0.60	2250	$22.08 \pm 0.29$
May 26.381	100.274	GEMINI/NIRI	K	0.60	2250	$> 22.25(3\sigma)$
Feb 26.552	11.446	GEMINI/GMOS	r	1.06	1800	$24.71 \pm 0.11$
Mar 8.394	21.287	GEMINI/GMOS	r	0.84	1800	$24.66 \pm 0.05$
June 10.287	115.180	GEMINI/GMOS	r	1.03	1800	$24.68 \pm 0.07$
Mar 11.530	-	GEMINI/GMOS	R400	-	7200	-

NOTE. — Log of photometry of XRF 050215B obtained at UKIRT and Gemini. The times given are the midpoint of the observations, errors quoted are  $1\sigma$ .

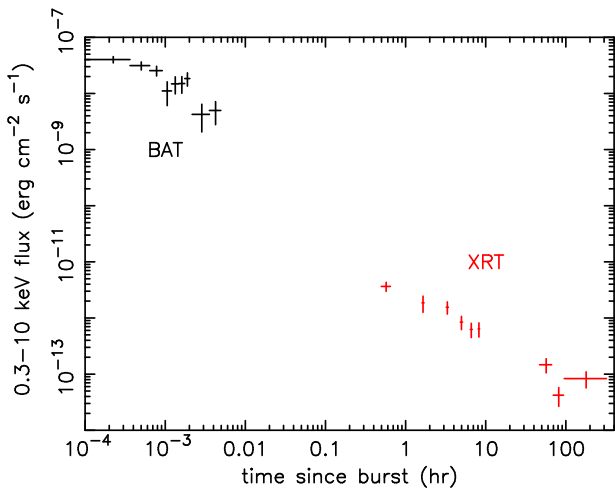


FIG. 3.— The joint BAT and XRT lightcurve of XRF 050215B. The XRT count-rates were converted into unabsorbed fluxes using the best fit model. The BAT data were extrapolated into the 0.3-10 keV band assuming a photon index which was the mean of the best-fit XRT and BAT spectral indices. The XRT data are best fit with an unbroken power-law with a decay index  $\alpha = 0.82 \pm 0.08$ . The extrapolation of the XRT observations to early times falls slightly below the prompt emission measured by the BAT (and the fitting of a single power-law to both BAT and XRT data does not result in a statistically acceptable fit, although given the calibration uncertainties it may be consistent with a single decline from  $10^{-3}$  hours onward). However, an extrapolation of the X-ray afterglow below the prompt emission could easily be explained by a steep decay of the X-ray flux at early times which is commonly seen in *Swift* bursts (e.g. Tagliaferri *et al.* 2005; Nousek *et al.* 2006; O’Brien *et al.* 2006).

ray and optical wavelengths. Although dust within the host galaxy could render the afterglow invisible at optical wavelengths and faint in the IR it could not simultaneously explain the faintness of the X-ray afterglow. Indeed an extrapolation of the X-ray afterglow into the optical/IR regime (using the method of Rol *et al.* 2005) reveals that for typical fireball parameters the observed K-band flux and optical limits are consistent with zero extinction. Unfortunately given the lack of multiband optical observations and the faintness of the X-ray afterglow excess absorption cannot be searched for either from the shape of the optical SED or by a decrement of soft X-rays.

An alternative model is that the burst lies at high red-

shift. Although it is now clear that some XRFs lie at low redshifts (e.g. XRF 020903 at  $z = 0.25$ , Soderberg *et al.* 2004), it is plausible that some fraction also originate in the very high redshift universe. The presence (and indeed brightness) of the host galaxy of XRF 050215B indicate that the redshift cannot be very high. However moderate luminosity distance (e.g.  $z > 2$ ) may still be a viable explanation of the faintness of the burst, although cannot explain the observed slow decay rate. Indeed *Swift* bursts are apparently fainter at all wavelengths than previous samples (Berger *et al.* 2005) and are also, on average, at significantly higher redshifts (a mean of  $z = 2.8$ ; Jakobsson *et al.* 2006). It is also interesting to note that the afterglow of XRF 050215B is significantly fainter than that of the high redshift GRBs 050904 ( $z = 6.29$  -Haislip *et al.* 2006; Price *et al.* 2005; Tagliaferri *et al.* 2005; Kawai *et al.* 2005) and GRB 050814 ( $z = 5.3$  Jakobsson *et al.* 2006).

The most popular models for the production of XRFs is that they are: (i) GRBs viewed away from the collimation axis (e.g. Yamazaki *et al.* 2002), (ii) bursts with high baryon contamination within the jet or (iii) bursts with jets which are intrinsically broader than those in GRBs. All of these models can efficiently soften the prompt emission from that seen in "classical" GRBs. Although the prompt emission of bursts from these different mechanisms may be largely indistinguishable, it is possible that their afterglows will show significant variation in their appearance (e.g. Granot *et al.* 2005). We consider these models, and how they may apply to the afterglow of XRF 050215B, below.

In the off-axis model, the highest energy emission (i.e.  $\gamma$ -rays) is confined within a narrow cone oriented slightly away from the observer and is not seen. The observed isotropic equivalent energy for these bursts ( $E_{iso}$ ) is thus lower than for bursts seen on axis and can reproduce the observed relationship between  $E_p$  and  $E_{iso}$  first reported by Amati *et al.* (2002). Granot *et al.* (2005) consider the afterglows produced by such a model. The early afterglow of a uniform jet with sharp edges can be seen to rise at early times as the more energetic material becomes visible; it then reaches a peak at a time roughly corresponding to the jet break, and from that point, follows a decay which is indistinguishable from an on-axis GRB (since all of the ejecta are visible), thus the late time decay slope would be expected to be rapid  $\sim t^{-p}$ . The

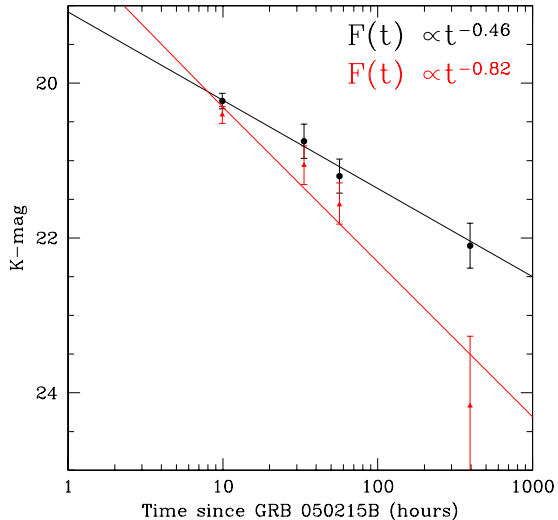


FIG. 4.— The K-band lightcurve of XRF 050215B obtained at UKIRT and Gemini. Also marked by a heavy line is the best fit power law decay  $F(t) \propto t^{-0.47}$ , which is very slow for GRB afterglows across this time frame. Also shown by triangles and a thin line is a putative host subtracted light curve (assuming that the host has  $K=22.25$ ). The thin line shows a (arbitrarily normalised) powerlaw with the same decay index as that seen in the X-ray lightcurve of XRF 050215B. As can be seen, within the uncertainty due to host subtraction it is possible that the K band decay has the same index as that seen in X-rays.

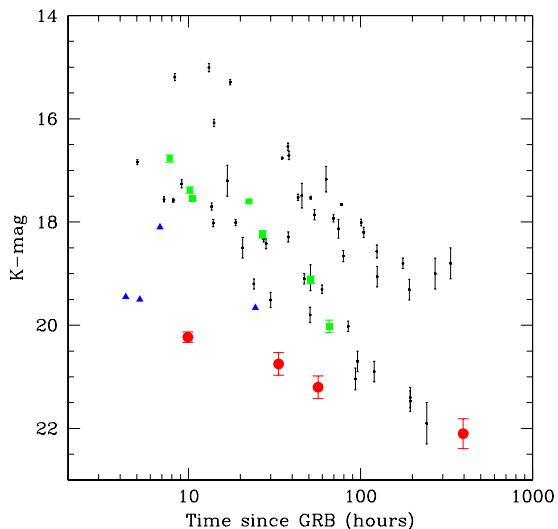


FIG. 5.— A comparison of the afterglow of XRF 050215B with the K-band afterglows of other GRBs (modified from that of Rau *et al.* 2004). The red circles are the afterglow of XRF 050215B, the blue triangles are for *Swift* bursts and the green boxes are for the high-redshift bursts. This plot shows that XRF 050215B has the faintest K-band afterglow yet seen. The data are taken from Rau *et al.* (and references therein) except for the more recent bursts which can be found in Berger *et al.* 2005; GRB 050401 Watson *et al.* 2005; GRB 050904 Haislip *et al.* 2006; Tagliaferri *et al.* 2005 and GRB 050814 Jakobsson *et al.* 2006.

afterglow of XRF 050215B does not show the rapid rise at early times which may be expected of off-axis models. However the rapid rise is a feature of jets with sharp edges. More realistic models which have smooth edges (either intrinsically or due to the interaction of the jet

with the stellar envelope) have a flat (but not necessarily rising) early lightcurve. Thus the early observations of XRF 050215B can be explained under this model. However, the late time slope should be steep ( $t^{-p}$ ) while a shallow slope is observed to 10 days post burst. Thus indicating that the jet must be moderately wide, although other GRBs (e.g. GRB 970508) have been shown to behave as a single power-law out to large times (see e.g. Bloom, Kulkarni & Frail 2003).

Under the dirty fireball model the XRF is produced by a jet which is viewed on-axis, but in which the Lorentz factor is reduced due to baryon loading. In this model the decay of the afterglow is much slower ( $f_\nu \propto t^{-3(p-1)/4}$  or  $f_\nu \propto t^{1/2-3p/4}$  depending of the location of the cooling break (Rhoads 2003)). Thus, for a typical  $p = 2$  burst the predicted decay slope would be  $t^{-0.75}$ , broadly consistent with the observed temporal slopes. However, dirty fireballs can only create a low peak energy if the prompt emission is created by external rather than internal shocks. Recent observations favour a scenario in which the bursts themselves are caused by internal shocks (Zhang *et al.* 2005). Furthermore the shape of the lightcurve, and comparison of the XRT and BAT lightcurves place constraints. In the dirty fireball model, the deceleration occurs when the outflow has collected  $1/\Gamma$  of rest mass; for lower values of  $\Gamma$  (i.e. XRFs) this deceleration time is significantly longer (scaling as  $\Gamma^{-8/3}$ ). The XRT observations cannot be used to constrain the deceleration time since they begin  $\sim 30$  minutes after the burst. However the shape of the BAT lightcurve implies that deceleration must have occurred at early times, and thus that the  $\Gamma$  cannot have been very low. Observations of future XRFs in X-rays in the seconds to minutes after the burst will allow stronger constraints to be made.

Alternatively, under the internal shock model a clean fireball can naturally accommodate the creation of an XRF (Zhang & Meszaros 2002), especially if the contrast in Lorentz factor between shells is small, which leads to inefficient energy dissipation (e.g. Barraud *et al.* 2004). In this case, the decay index of  $\alpha = 0.82$  can also naturally be accommodated, although only if it is observed prior to the jet-break.

A final possibility is that the XRF is caused by the opening angle of the jet itself. Broad jets in GRBs may be present either alone (e.g. Lamb, Donaghy & Graziani, 2005) or as a multicomponent structure including narrower ( $\gamma$ -ray emitting) jets (e.g. Berger *et al.* 2003; Huang *et al.* 2004), although such models have recently been shown not to fit the afterglow of GRB 030329, which they were posited to explain (Granot 2005). These broader jets have correspondingly later jet break times than the narrow emission responsible for the GRB, and would naturally explain the lack of a jet break for  $>10$  days after the burst. Indeed, regardless of the precise mechanism for the generation of this XRF, the lack of jet break implies that the jet opening angle must be wide, perhaps making a broader jet the most likely explanation.

It is also interesting to compare the properties of both the prompt and X-ray emission of XRF 050215B with those of the population of bursts detected by *Swift*. Although the *HETE-2* observations allowed for this burst to be classified as an XRF, the behaviour as observed by

the BAT was not significantly different from that seen in many other bursts. Indeed the measured photon index of 2.0 is comparable to the mean of *Swift* bursts in general (e.g. O’Brien *et al.* 2006), although it does lie amongst the softer bursts detected by BATSE (as do many *Swift* GRBs). Thus, it may be that *Swift*, as for *HETE-2* and *BeppoSAX*, does detect a large population of XRFs. However, *Swift* is unable to accurately constrain their spectral properties due to its limited bandpass in comparison to previous missions. Indeed in the case of XRF 050406 the apparent peak energy  $E_p < 15\text{keV}$  (Romano *et al.* 2005) and thus although it was possible to identify the burst as an XRF its peak energy and detailed spectral prompt spectral properties could not be accurately measured. Only XRF 050416 has a measured  $E_p$  from *Swift*, with  $E_p = 15.6\text{keV}$  (Sakamoto *et al.* 2005). However, even in this case the measurement is relatively weak, since a simple power-law fit yields a  $\chi^2/dof < 1$ .

The afterglow of the burst is both fainter than typical (even for *Swift* bursts) and also more slowly declining, with no evidence for a jet break during long observations lasting for 10 days since the burst. The afterglow is very faint in the K-band (fainter than the majority of upper limits on K-band afterglow brightness) and lies at the faint end of the flux distribution for long duration GRB detected by *Swift*. There are a number of comparably faint bursts e.g. GRB 050223 - Page *et al.* 2005; GRB/XRF 050406 - Romano *et al.* 2005; GRB 050421 - Godet *et al.* 2006, GRB 050911 - Page *et al.* 2006. It is interesting to note that the proposed explanations for this faintness vary widely, demonstrating the large range of physical processes which affect the brightness of a given afterglow. For example GRB 050911 was interpreted as being due to a BH-NS merger, since its lack of an X-ray afterglow was reminiscent of short duration GRBs (e.g. Gehrels *et al.* 2005), while its lightcurve could also be interpreted as being due to several accretion event which are seen in BH-NS mergers (Davies, Levan & King 2005). In contrast GRB 050421 was explained as being due to a "naked" GRB - a burst occurring in a region of very low density, which thus affected the brightness of the afterglow (e.g. Taylor *et al.* 2000). For XRFs, such explanations are not normally considered and the most commonly discussed explanations involve differing geometries of either the jet itself or the observer orientation. For example the flat slopes of the afterglow lightcurves are predicted in various off-axis models. However, for "normal" long duration bursts a generic feature of the afterglow light curve is a flat phase in the afterglow (e.g. Nousek *et al.* 2005). This is normally interpreted as being due to late time energy injection from the central engine, and is also interpreted as such in the afterglow of XRF 050406 (Romano *et al.* 2005), which has a very flat light curve out to late times  $\alpha \sim 0.5$ . While this flat phase is obviously a generic feature of X-ray afterglows it is less apparent in the optical and IR. Thus for XRF 050215B, where the X-ray and optical decays are similar it is more likely that the relatively slow decay is simply a result of the jet structure. It is also interesting to note that other optical afterglows of XRFs have shown similar behaviour to XRF 050406 in the optical regime. For example XRF 020903 showed flaring behaviour and a flat decay in the R-band (Bersier *et al.* 2006), behaviour which has not commonly been seen in GRB afterglows

(although the sample of XRF optical/IR afterglows remains much smaller).

One of the most important contributions that *Swift* has made to the GRB field comes from the decrease in time between the burst itself and the first pointed observations. Although in the pre-*Swift* era a few bursts were observed promptly in the optical (e.g. GRB 990123, Akerlof *et al.* 1999) these were rare, and prompt, pointed, X-ray observations were never made. It was thus hoped that the early afterglow emission would provide crucial tests of various afterglow models. In practice, the behaviour seen is somewhat different from what was expected (e.g. Tagliaferri *et al.* 2005; Nousek *et al.* 2005), and the presence of frequent X-ray flares (e.g. Burrows *et al.* 2005) makes the X-ray afterglows a less "clean" probe than may have been hoped for. Nonetheless, this early phase can provide powerful diagnostics of various models. O’Brien *et al.* (2006) have studied this transition period for a number of GRBs and show that generally the extrapolation of the X-ray afterglow to early times "joins" with the prompt emission and does not exhibit a strong discontinuity. This behaviour, when seen in XRFs, disfavors a sharp-edged jet if jet geometry is the dominating factor. However, for three well studied *Swift* X-ray afterglows (XRF 050215B, XRF 050406 and XRF 050416) there is apparently no jet break seen out to late times ( $> 10$  days in each case). Thus, all of these cases must have wide opening angles. Ultimately, insight into the XRF phenomena is likely to be made via the subset of bursts which are detected simultaneously by BAT and another satellite (e.g. HETE-2, Suzaku-WAM, Konus) and where early X-ray and optical observations can be paired with well constrained spectral parameters for the prompt emission.

#### 4. CONCLUSIONS

We have presented observations of XRF 050215B. This was the first X-ray Flash to be located by *Swift* and was achieved by the use of *HETE-2* and *Swift* in synergy, utilising the sensitivity and wide field of view of the *Swift*-BAT and the wide spectral range of *HETE-FREGATE*. The fluence within the prompt emission was comparable to that seen in previous XRFs, although the X-ray lightcurve is fainter than the majority of *Swift* bursts, while in the infrared XRF 050215B is the faintest afterglow ever to have been detected (although some bursts have been invisible to comparable limits). Indeed, XRF 050215B had a flux at 9 hours which was only just observable with a 4m telescope, and at early times was invisible to any robotic or UVOT observations. As also suggested by Berger *et al.* (2005), this implies that locating the afterglows of some GRBs in the *Swift* era will require rapid response observations from larger telescopes since many bursts will be too faint to be detected by the UVOT or even by larger aperture robotic ground based telescopes.

The limited volume of data and lack of redshift available for this burst make it difficult to draw firm conclusions as to the cause of the soft  $\gamma$ -ray spectrum; however the lack of any observed jet-break to  $> 10$  days post burst make a broad jet the most likely explanation. The late-time behaviour of XRF 050215B is qualitatively somewhat similar to the late-time X-ray lightcurve of the recent GRB 060218, which, by virtue of its proximity (145

Mpc) had a bright X-ray and Optical afterglow. In particular, GRB 060218 also had a long-lasting slow decay, as seen in XRF 050215B, although the relative faintness of both afterglow and host galaxy, coupled with the lack of any supernova emission, imply a much higher redshift in the latter case. Furthermore GRB 060218 had an ex-

ceptionally long duration in  $\gamma$ -rays ( $t_{90} \sim 2000$ s), making the status of GRB 060218 relative to the bulk of the XRF population unclear, and pointing to the continuing need for further well-observed XRFs if we are to understand the diversity in their emission mechanisms and their relationship to GRBs.

## REFERENCES

- Amati, L. et al. 2002, *A&A*, 390, 81  
 Barraud, C., Daigne, F., Mochkovitch, R., & Atteia, J. L. 2005, *A&A*, 440, 809  
 Barthemly, S. et al. 2004, *SPIE* 5165, 175  
 Barthemly, S. et al. 2005a, *GCN* 3024  
 Barthemly, S. et al. 2005b, *Space Science Reviews*, 120, 143  
 Berger, E., et al. 2003, *Nature*, 426, 154  
 Berger, E., et al. 2005, *ApJ*, 629, 328  
 Bersier, D., et al. 2006, *ArXiv Astrophysics e-prints*, arXiv:astro-ph/0602163  
 Bloom, J.S. et al. 2003, *ApJ*, 599, 957  
 Bloom, J. S., Frail, D. A., & Kulkarni, S. R. 2003, *ApJ*, 594, 674  
 Burrows, D. et al. 2004, *SPIE*, 5165, 201  
 Burrows, D. et al. 2005, *Space Science Reviews*, 120, 165  
 Burrows, D. N., et al. 2005, *Science*, 309, 1833  
 Butler, N. R., et al. 2005, *ApJ*, 621, 884  
 Campana, S., et al. 2006, submitted to *Nature*, astro-ph/0603279  
 Cavanagh, B., Hirst, P., Jenness, T., Economou, F., Currie, M. J., Todd, S., & Ryder, S. D. 2003, *ASP Conf. Ser.* 295: *Astronomical Data Analysis Software and Systems XII*, 295, 237  
 Chary, R., Becklin, E.E., Armus, L. 2002, *ApJ*, 566, 229  
 Dado, S., Dar, A., & De Rujula, A., 2004, *A&A*, 422, 381  
 Davies, M. B., Levan, A. J., & King, A. R. 2005, *MNRAS*, 356, 54  
 Dermer, C.D., Chiang, J., & Bottcher, M. 1999, *ApJ*, 513, 656  
 Fynbo, J. et al. 2004, *ApJ*, 609, 962  
 Gehrels, N., et al. 2004, *ApJ*, 611, 1005  
 Gehrels, N., et al. 2005, *Nature*, 437, 851  
 Goad, M. et al. 2005, *GCN* 3034  
 Granot, J., Ramirez-Ruiz, E., & Perna, R. 2005, *ApJ*, 630, 1003  
 Granot, J. 2005, *ApJ*, 631, 1022  
 Haislip, J. B., et al. 2006, *Nature*, 440, 181  
 Heise, J. et al in *Gamma-Ray Bursts in the Afterglow Era*, ed E. Costa, F. Frontera, F. Frontera & J. Hjorth (Berlin: Springer), 16  
 Hjorth, J., et al. 2003, *Nature*, 423, 84  
 Hodapp, K.-W. et al. 1995, *PASP*, 115, 1388  
 Hook, I. et al. 2004, *PASP*, 116, 425  
 Huang, Y. F., Dai, Z. G., & Lu, T. 2002, *MNRAS*, 332, 735  
 Huang, Y. F., Wu, X. F., Dai, Z. G., Ma, H. T., & Lu, T. 2004, *ApJ*, 605, 300  
 Jakobsson, P., et al. 2006, *A&A*, 447, 897  
 Jelinek et al. 2005, *GCN* 3029  
 Kippen, R.M. et al. 2003, *AIP Conf Proc*, 662, 244  
 Kouveliotou, C., et al. 2004, *ApJ*, 608, 872  
 Le Floc'h, E. et al. 2003, *A&A*, 400, 499  
 Levan, A. et al. 2005, *ApJ*, 622, 977  
 Mészáros, P., Ramirez-Ruiz, E., Rees, M. J., Zhang, B. 2002, *ApJ*, 578, 812  
 Modjaz, M., et al. 2006, *ArXiv Astrophysics e-prints*, arXiv:astro-ph/0603377  
 Moretti, A., Perri, M., Capalbi, M., Angelini, L., Hill, J. E., Campana, S., Burrows, D. N., & Osborne, J. P. 2005, *ArXiv Astrophysics e-prints*, arXiv:astro-ph/0511604  
 Nakagawa, Y. et al. 2005, *GCN* 3053  
 Nousek, J. A., et al. 2005, *ArXiv Astrophysics e-prints*, arXiv:astro-ph/0508332  
 O'Brien, P. T., et al. 2006, *ArXiv Astrophysics e-prints*, arXiv:astro-ph/0601125  
 Page, K. L., et al. 2005, *MNRAS*, 363, L76  
 Page, K. L., et al. 2006, *ApJ*, 637, L13  
 Pian, E., et al. 2006, submitted to *Nature*, astro-ph/0603530  
 Price, P. A., Cowie, L. L., Minezaki, T., Schmidt, B. P., Songaila, A., & Yoshii, Y. 2005, *ArXiv Astrophysics e-prints*, arXiv:astro-ph/0509697  
 Ramirez-Ruiz, E., Lloyd-Romring, N., 2002, *NewA*, 7, 197  
 Rau, A., et al. 2004, *A&A*, 427, 815  
 Rhoads, J. E., 2003, *ApJ*, 591, 1097  
 Roche, P.F. et al. 2002, *SPIE*, 4841, 901  
 Rol, E. et al. 2005, *ApJ*, 624, 868  
 Romano, P., et al. 2006, *ArXiv Astrophysics e-prints*, arXiv:astro-ph/0601173  
 Roming, P. et al. 2004, *SPIE*, 5165, 262  
 Roming, P. et al. 2005a, *GCN* 3026  
 Roming, P. et al. 2005b, *GCN* 3069  
 Roming, P. et al. 2005c, *Space Science Reviews*, 120, 95  
 Sakamoto, T., et al. 2005, *ApJ*, 629, 311  
 Sakamoto, T., et al. 2006, *ApJ*, 636, L73  
 Sazonov, S. Y., Lutovinov, A. A., & Sunyaev, R. A. 2004, *Nature*, 430, 646  
 Schady, P., et al. 2006, *ArXiv Astrophysics e-prints*, arXiv:astro-ph/0601182  
 Soderberg, A.M. et al. 2004a, *ApJ*, 606, 994  
 Soderberg, A. M., et al. 2005, *ApJ*, 627, 877  
 Soderberg, A., Frail, D. 2005a, *GCN* 3035  
 Soderberg, A., Frail, D. et al. 2005b, *GCN* 3066  
 Stanek, K. Z., et al. 2003, *ApJ*, 591, L17  
 Tagliaferri, G., et al. 2005, *A&A*, 443, L1  
 Tagliaferri, G., et al. 2005, *Nature*, 436, 985  
 Taylor, G. B., Bloom, J. S., Frail, D. A., Kulkarni, S. R., Djorgovski, S. G., & Jacoby, B. A. 2000, *ApJ*, 537, L17  
 Tanvir et al. 2005a, *GCN* 3031  
 Watson, D., et al. 2005, *ArXiv Astrophysics e-prints*, arXiv:astro-ph/0510368  
 Yamazaki, R., Ioka, K. & Nakamura, T., 2002, *ApJ*, 571, L31  
 Yost, S. A., Smith, D. A., & Rykoff, E. S. 2005, *GRB Coordinates Network*, 3022, 1  
 Zhang, B., & Mészáros, P. 2002, *ApJ*, 581, 1236  
 Zhang, W., Woosley, S.E., Heger, A., 2004, *ApJ*, 608, 365  
 Zhang, B., Fan, Y. Z., Dyks, J., Kobayashi, S., Meszaros, P., Burrows, D. N., Nousek, J. A., & Gehrels, N. 2005, *ArXiv Astrophysics e-prints*, arXiv:astro-ph/0508321